ESOMAT 2009, 06008 (2009)
DOI:10.1051/esomat/200906008

Numerical simulation of Nitinol peripheral stents: from laser-cutting to deployment in a patient specific anatomy

Michele Conti[1,2,a], Ferdinando Auricchio[1], Matthieu De Beule[2], and Benedict Verhegghe[2]

[1] Structural Mechanics Department, Universitá degli Studi di Pavia, Pavia, Italy
[2] Institute Biomedical Technology (IBiTech), Faculty of Engineering, Ghent University, Ghent, Belgium

Abstract. The current clinical trend is to use percutaneous techniques, exploiting Nitinol self-expanding stents, to treat peripheral occluded vessels such as carotid or superficial femoral arteries. Although this class of stents addresses the biomechanical requirements (i.e. flexibility, kink resistance, etc.), it has been observed that many of these stents implanted in peripheral vessels are fractured. Numerical simulations have shown to be very useful in the investigation and optimization of stents and also to provide novel insights into fatigue/fracture mechanics. To date most finite element based stent simulations are performed in a straight simplified anatomy and neglect the actual deployment process; consequently there is a need for more realistic simulations taking into account the different stages of the stent design process and the insertion in the target anatomy into account. This study proposes a virtual framework to analyze numerically Nitinol stents from the laser-cutting stage to the deployment in a (patient specific) tortuous anatomy.

1 Introduction

Cardiovascular disease (CVD), which is often related to atherosclerosis, is the most common cause of death in European countries [1]. Current trend in clinical practice is to treat peripheral vascular districts, such as carotid or superficial femoral artery, using percutaneous techniques exploiting Nitinol self-expanding stents.
In the highly deformable peripheral arteries, the in-vivo stress-state is multi-axial and complex [2] and the vessel anatomy is tortuous and non-homogeneous. Thanks to the peculiar features of Nitinol, this class of stents accomplishes both technical and biomechanical requirements (i.e. flexibility, kink resistance, low delivery profile etc.); unfortunately it has been observed that many of these stents implanted in peripheral vessels are fractured [3]-[4].
Currently, several peripheral stent designs are available on a dedicated, fast-growing market exhibiting a variable ability to withstand chronic deformation depending on stent design and the type of applied deformation [5], moreover many stent designs are designed only to survive under a standard pulsatile fatigue environment.
Numerical simulations have shown to be a very useful tool in the investigation and optimization of stent design [6]-[7] and to provide novel insights on fatigue/fracture mechanics [8].
To date few finite element analyses (FEA) of Nitinol stent implant simulations are available and most of them consider straight simplified anatomy and neglect the actual deployment process; only recently some study has been proposed to accomplish more realistic simulation of

[a] e-mail: michele.conti@unipv.it

Article available at http://www.esomat.org or http://dx.doi.org/10.1051/esomat/200906008

peripheral stenting [9]-[10].
Consequently there is still a need for more realistic simulations taking the different stages of the Nitinol stent design process and the insertion in the target anatomy into account.
This study proposes a software framework, coupling pyFormex [11] and Abaqus [12], allowing to analyze numerically a stent design from the laser-cutting stage to its deployment in patient specific carotid artery model. In particular, for demonstration purpose, the present study shows the application of the computational framework to a tapered XACT stent (Abbott, Illinois, USA), a closed cell stent design used to treat carotid stenosis.

2 Materials and Methods

The proposed computational framework takes into account two main steps in order to simulate the whole work flow (represented in Fig. 1) characterizing the stent design forming and its subsequent implant:

1. creation of 3D parametric finite element (FE) model of a laser-cut stent and its expansion before heat treatment (stent forming);
2. crimping/bending of the expanded stent mimicking the stent insertion by the delivery system and gradual deployment of the stent within the curved vessel (stent implant).

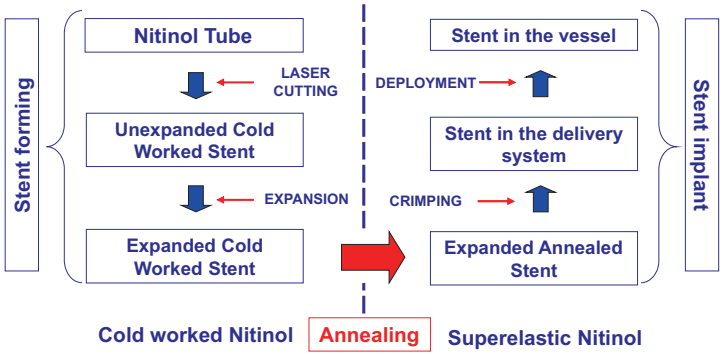

Fig. 1. Main steps of process leading from stent manufacturing to its delivery.

Within the computational framework, pyFormex is used to create directly the complete input files for the FE solver (ABAQUS Explicit). In particular pyFormex is exploited to create the stent mesh; in fact it allows for an easy definition of a parametric mesh accounting for several stent features (i.e. stent radius, stent length, number of rings, number of bridges, strut thickness, etc.) [13]. The stent mesh is combined with a cylinder mimicking the rigid expander used for the shape setting, leading from laser-cut to expanded stent configuration, before the heat treatment. The stent mesh consisted of 93024 linear hexahedral reduced integration (C3D8R) elements. The cylinder mesh consisted of 800 three-dimensional, 4-node surface element with reduced integration (SFM3D4R).
At this stage, before annealing, the mechanical behavior of cold-worked Nitinol is similar to usual metals, like aluminum or common steel; consequently for this simulations Nitinol is modeled as an elasto-plastic material using the material parameters based on the work of Theriault et al. [14].
During the simulation, the cylinder expansion and the consequent stent diameter increase has been imposed applying appropriate boundary conditions on the rigid cylinder mesh. The simulation performed in this step provides the expanded stent configuration as shown in Fig. 2.

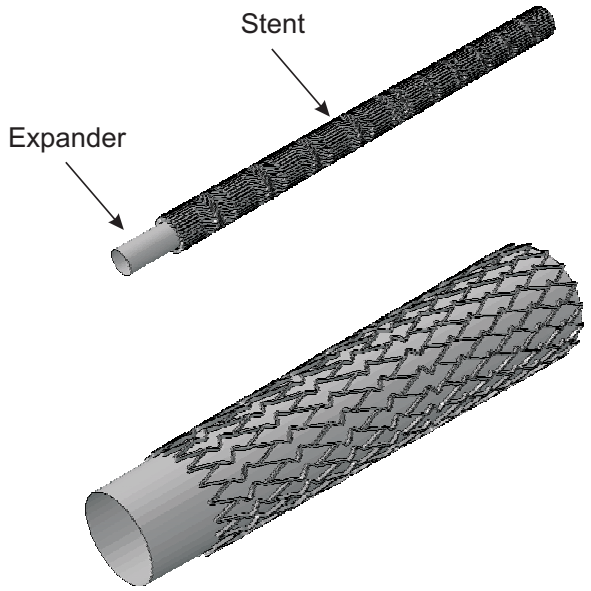

Fig. 2. Unexpanded stent (on top); Expanded stent (on bottom).

Subsequently to perform the simulation of stent implantation, the stent mesh obtained from the previous simulation is re-imported in Abaqus and combined with the catheter and vessel mesh.
The FE model of the carotid artery is generated by means of Go-Mesh [15] elaborating patient specific geometrical information available on line (www.charite.de). The vessel mesh consists of 78330 10-node modified tetrahedrons, with hourglass control (C3D10M). No atherosclerotic plaque is considered in the model.
To reproduce the superelastic material response, we use the Abaqus implementation VUMAT [16] of the superelastic model originally proposed by Auricchio and Taylor [17]-[18] and based on the concept of generalized plasticity [19].
The theory decomposes strain into two parts: a purely elastic component $\Delta\epsilon^{el}$ and a transformation component $\Delta\epsilon^{tr}$

$$\Delta\epsilon = \Delta\epsilon^{el} + \Delta\epsilon^{tr} \tag{1}$$

The transformation from austenite to twinned martensite is driven by the resolution of shear forces taking place within a range of stress thresholds, which are characteristic of the material

$$\Delta\epsilon^{tr} = a\Delta\zeta\frac{\partial F}{\partial\sigma} \tag{2}$$

$$F^S \leq F \leq F^F \tag{3}$$

where ζ is the fraction of martensite and F is the transformation potential.
The same principle is applied to define the reverse transformation taking into account different stress thresholds.
The transformation intensity is defined by the following law:

$$\Delta\zeta = f(\sigma,\zeta)\Delta F \tag{4}$$

Any changes in stress direction produces a martensite reorientation with a negligible additional effort. Moreover the model includes a shift of stress thresholds as linear function of the temperature.
Since there is a volume increase related to to the transformation, less stress is required to produce transformation in tension and more in compression; such an effect is modeled by a linear Drucker-Prager approach for the transformation potential:

$$F = \bar{\sigma} - ptan(\beta) + cT \tag{5}$$

with $\bar{\sigma}$ is the Mises equivalent stress, p the pressure stress, and T the temperature, c and β material constants. The adopted Nitinol constitutive parameters, reported in Table 1, are obtained from literature [20].

Table 1. adopted Nitinol constitutive parameters [20].

Symbol	Description	Value
E_A	Austenite elasticity	51700 MPa
ν_A	Austenite Poisson's ratio	0.3
E_M	Martensite elasticity	47800 MPa
ν_M	Martensite Poisson's ratio	0.3
ϵ^L	Transformation strain	0.063
$(\partial\sigma/\partial T)_L$	stress/temperature ratio during loading	6.527
σ_L^S	Start of transformation loading	600 MPa
σ_L^E	End of transformation loading	670 MPa
T_0	Reference temperature	37^o
$(\partial\sigma/\partial T)_U$	stress/temperature ratio during unloading	6.527
σ_U^S	Start of transformation unloading	288 MPa
σ_U^E	End of transformation unloading	254 MPa

Moreover vessel tissue is modeled as an isotropic hyperelastic material [21].
During the simulation, in a first stage, the catheter is crimped and bent accomplishing the curved configuration of the vessel leading to stent deformation while the contact between the stent and the vessel is deactivated.
In a second stage, the contact between the stent and the vessel is activated while the catheter is gradually re-expanded accomplishing stent expansion and its apposition and the subsequent complete stent apposition to the vessel wall.

3 Results and Conclusions

The results of the Nitinol stent implant simulation are reported in Fig. 3. The stent, exploiting the Nitinol superelastic effect is able to recover its tapered shape after the release; the original tortuous vessel shape is clearly influenced by the interaction with the stent; in particular the simulation shows that the analyzed design straightens the vessel considerably having consequently a limited flexibility.
Computer modeling can play an important role in the design of medical devices and in the investigation of their mechanics. In the present study, a computational framework to numerically investigate the forming and implant of Nitinol laser-cut stents is presented. This study can represent a first step for further parametric studies and more complex and realistic simulations. Further investigation can include the comparison of different stent designs and configurations and the related impact on vessel anatomy.

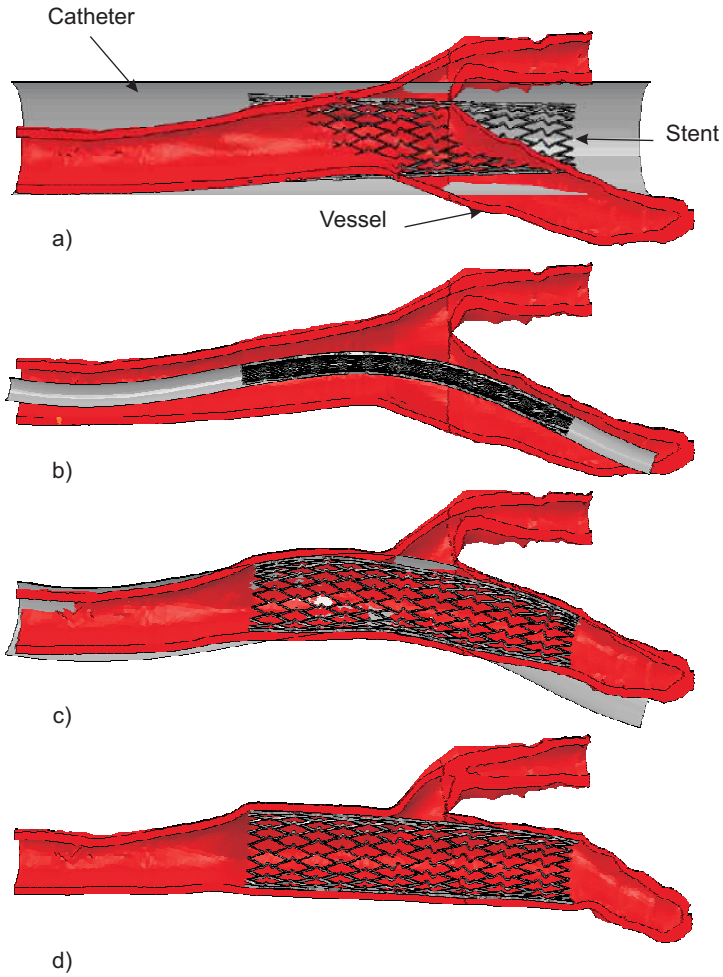

Fig. 3. Simulation of stent implant in carotid artery: a) starting configuration of the FE model; b) stent crimped in the delivery system; c) partially deployed stent; d) stent deployed in the vessel.

References

1. Petersen S., Peto V., Rayner M., Leal J., Luengo-Fernandez R. and Gray A., 2005, *European Cardiovascular Disease Statistics*, BHF London
2. Smouse H.B., Nikanorov A. and LaFlash D., 2005, *Biomechanical Forces in the Femoropopliteal Arterial Segment What happens during extremity movement and what is the effect on stenting?*, Endovascular Today, June, pp. 60-66
3. Allie D.E., Hebert C.J., Walker C.M., 2004, *Nitinol stent fractures in the SFA*, Endovascular Today, Jul/Aug, pp. 22-34
4. Scheinert D., Scheinert S., Sax J., Piorkowski C., Brunlich S., Ulrich M., Biamino G., Schmidt A., 2005, *Prevalence and clinical impact of stent fractures after femoropopliteal stenting*, J Am Coll Cardiol, 45, pp. 312-315
5. Nikanorov A., Smouse H.B., Osman K., Bialas M., Shrivastava, and Schwartz B., 2008, *Fracture of self-expanding nitinol stents stressed in vitro under simulated intravascular conditions*, 48, pp. 435-40

6. Auricchio F., Di Loreto M., Sacco E., 2000, *Finite element analysis of a stenotic artery revascularization through stent insertion*, Comp Meth Biomech Biomed Eng, 0, pp. 1-15
7. De Beule M., Mortier P., Carlier S.G., Verhegghe B., Van Impe R., Verdonck P., 2008, *Realistic finite element-based stent design: The impact of balloon folding*, Journal of Biomechanics, 41(2), pp. 383-9
8. Marrey R. V., Burgermeister R., Grishber R.B, Ritchie R.O., 2006, *Fatigue and life prediction for cobalt-chromium stents: A fracture mechanics analysis*, Biomaterials, 27, pp. 1988-2000
9. Rebelo N., Fu R., and Lawrenchuk M., 2009, *Study of a Nitinol Stent Deployed into Anatomically Accurate Artery Geometry and Subjected to Realistic Service Loading*. Journal of Materials Engineering and Performance. doi: 10.1007/s11665-009-9375-0.
10. Wu W., Qi M., Liu X.P., Yang D.Z., Wang W.Q., 2007, *Delivery and release of nitinol stent in carotid artery and their interactions: A finite element analysis*, Journal of Biomechanics, 40, pp. 3034-3040
11. Internet site address: http://pyFormex.berlios.de
12. Dassault Systémes Simulia Corp., Providence, RI, USA
13. Mortier P., De Beule M., Van Loo D., Verdonck P., Verhegghe B., 2008, *Parametric Stent Design Using pyFormex*, Proceedings of the ASME 2008 Summer Bioengineering Conference (SBC2008). June 25-29, Marriott Resort, Marco Island, Florida, USA
14. Thériault P., Terriault P., Brailovski V., Gallo R., 2006, *Finite element modeling of a progressively expanding shape memory stent*, Journal of Biomechanics, 39, pp. 2837-2844
15. Internet site address: http://we.gomesh.it/
16. Rebelo N., Walker N., and Foadian H., 2001, *Simulation of implantable stents*, Abaqus User's Conference 2001, pp. 421-434
17. Auricchio F., Taylor R., 1996, *Shape-memory alloys: modeling and numerical simulations of the finite-strain superelastic behavior*, Comput. Methods. Appl. Mech. Engng., 143, pp. 175-94
18. Auricchio F., Taylor R., 1997, *Shape-memory alloys: macromodeling and numerical simulations of the superelastic behavior*, Comput. Methods. Appl. Mech. Engng., 146, pp. 281-312
19. Lubliner J., Auricchio F., 1996, *Generalized plasticity and shape memory alloy*, Int. J. Solids. Struct. 33, pp. 991-1003
20. Kleinstreuer C., Li Z., Basciano C.A., Seelecke S., and Farber M.A., 2008, *Computational mechanics of Nitinol stent grafts*, Journal of Biomechanics, 41, pp. 2370-2378
21. Lally C., Dolan F., and Prendergast P., 2005, *Cardiovascular Stent Design and Vessel Stresses: a Finite Element Analysis*, Journal of Biomechanics, 38(8), pp. 1574-1581